A Thin Viscous Sheet Model for Continental Deformation

William Davis

Saturday 16th December, 2017

Introduction

Continental collision produces some of the most striking tectonic features on the Earth?s surface. The collision of the Indian tectonic plate into Asia at 60 Ma caused the formation of the Himalayan range and surrounding Tibetan Plateau, the highest elevation on Earth. This process caused huge amounts of uplift and crustal thickening over a far horizontal extent. To better understand this process, numerical models can be used to test mechanisms and physical properties. In this study, I attempt to reproduce the models of England and McKenzie, 1982 [1]. Appropriate corrections and changes are made according to later publications [2].

Theory

The general theory behind the thin viscous sheet approximation is that the crust is represented as a thin layer that is isostatically in equilibrium with the lithosphere, and velocities within the crust do not vary with depth. This flow is incompressible and is driven by tractions and the gradients in crustal thickness. Vertical gradients of deviatoric stresses are also neglected. Considering vertical gradients in forces and rheology, it can be shown:

$$p = \tau_{zz} - \int_0^z \rho g dz' \tag{0.1}$$

Considering a level at the base of the lithosphere for isostatic balence ($z = 0$). The vertical average of this pressure through the lithosphere and any topography gives:

$$\bar{p} = \bar{\tau}_{zz} - \frac{g\rho_c}{2L}(1 - \rho_c/\rho_m)S^2 + \frac{g\rho_m L}{2} \tag{0.2}$$

The term $\bar{\tau}_{zz}$ is calculated through the constitutive equation:

$$\bar{\tau}_{zz} = B\dot{E}^{(\frac{1}{n}-1)}\dot{\varepsilon_{ij}} \tag{0.3}$$

This describes power-law rheology, where $n = 1$ is a Newtonian fluid. The parameter B is a constant which encompasses depth averaged viscosity, and $\dot{E}$ is the second invariant of the strain rate tensor.

Substituting (xx) and (xx) into force-balance equations in the horizontal directions (derived from the equation $\frac{\partial \sigma_{ij}}{\partial x_j} = \rho g a_i$), gives:

$$\nabla^2 u = -3\nabla(\nabla \cdot u) + 2(1-1/n)\dot{E}^{-1}\left[\nabla\dot{E}\cdot\dot{\varepsilon_{ij}} + (\nabla\cdot u)\nabla\dot{E}\right] + 2Ar\dot{E}^{(1-\frac{1}{n})}S\nabla S \tag{0.4}$$

In this representation, only horizontal derivatives are considered. The terms are non-dimensional and the Argand number (Ar) is defined as:

$$Ar = \frac{g\rho_c(1-\rho_c/\rho_m)L}{B(u_0/L)^{1/n}} \tag{0.5}$$

This number describes the relative contributions of forces arising from variations in crustal thicknesses and the force required to deform a fluid. For large Ar, the crustal gravitational forces succumb to deformation - the lithosphere is weak (a tyrological analogue might be a ripe brie). Small Ar flows resist deformation and changes in crustal thickness, forming rigid blocks (think feta).

The continuity equation may be written in the form:

$$\frac{\partial s}{\partial t} = -\nabla\cdot(su) \tag{0.6}$$

... to constrain time-dependence.

COMPUTATION AND IMPLEMENTATION

Equations are solved on a 32x32 grid, through numerical approximations to equations (0.4) and (0.6). The derivative terms in the RHS of equation (xx) are approximated through centre difference schemes.

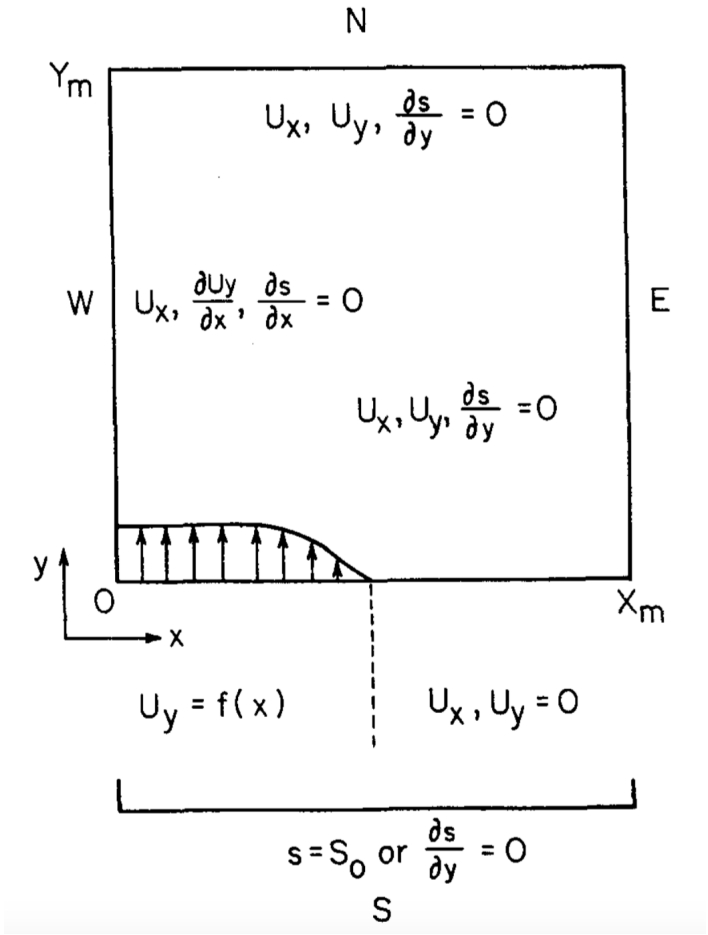

Figure 1: Geometry of numerical model.

To solve for the velocity field on the LHS, the interior nodes of the RHS are initially set to zero and the new velocity field is inverted for using a Poisson solving routine.

$$\nabla^2 u = f(x, y) \tag{0.7}$$

Boundary conditions are then applied to the velocity fields. These new velocity fields are then used in the centre difference schemes to calculate a new RHS, which is solved again to attain a new solution for the velocities (again applying boundary conditions). This new solution is added to the old solution:

$$u_{new} = \alpha u_{current} + (1 - \alpha) u_{old} \tag{0.8}$$

For calculations, very small values for α must be used (about 1×10^{-3}). This is iterated on until the maximum difference in either velocity field is lower than a critical value (2.5×10^{-3} was used).

To advance the solution in time, as well as calculate changes in crustal thickness, approximations to equations (0.6) are used. The LHS is approximated be a forward difference, and the RHS is approximated using an 'upwind' scheme, as the form of equation (xx) lends similarities to a material derivative. Timesteps are chosen to be small so they satisfy the Courant-Friedrichs-Lewy criterion.

RESULTS

Preliminary results indicate that numerical simulations with similar resolution to the original study can be performed very quickly - simulations were performed on a laptop and took less than 5 minutes even at high Ar values. Only variations in Argand number were explored, as n (power law rheology) was kept constant at 1.

LOW ARGAND NUMBER

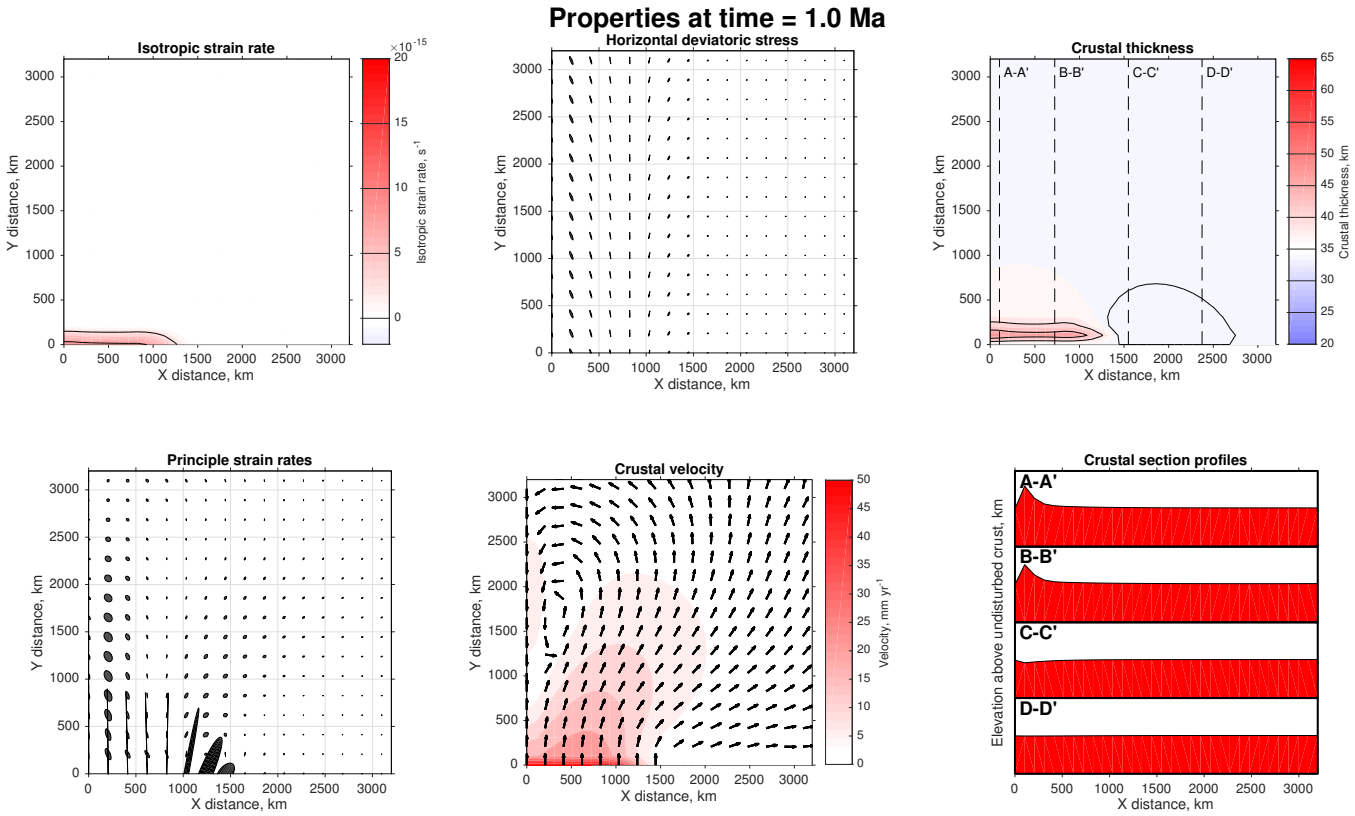

Figure 2: Results from numerical models illustrating velocity, strain, differential stress, and crustal thickness. Simulations performed at Ar=1, n=1, for 1 Myrs. Parameters are calculated on a 32x32 grid and displayed as colours or every 2L spacings, where appropriate. Top-left: Isotropic strain rate field calculated from instantaneous thickening or thinning: $-(\varepsilon_{xx}+\varepsilon_{yy})$ for the velocity field. Bottom-left: Directions and relative magnitudes of principle shear strain rates for the flow. Top-middle: Directions and relative magnitudes of principle horizontal deviatoric stresses for the flow. Bottom-middle: Velocity field for the flow. Magnitude of velocity is shown as a background colour, and directions are indicated by arrows. Top-right: Crustal thickness resulting from flow. Bottom-right: Sections of crustal thicknesses as indicated from top-right plot.

Simulations with low Argand numbers (Figures 2 and 3) show a concentration short range in crustal thickening between 1 and 5 Myrs. Thickening ranging from 500-1000km from the indented corner is observed. In addition, there is a slight crustal thinning observed about 2000 km along strike.

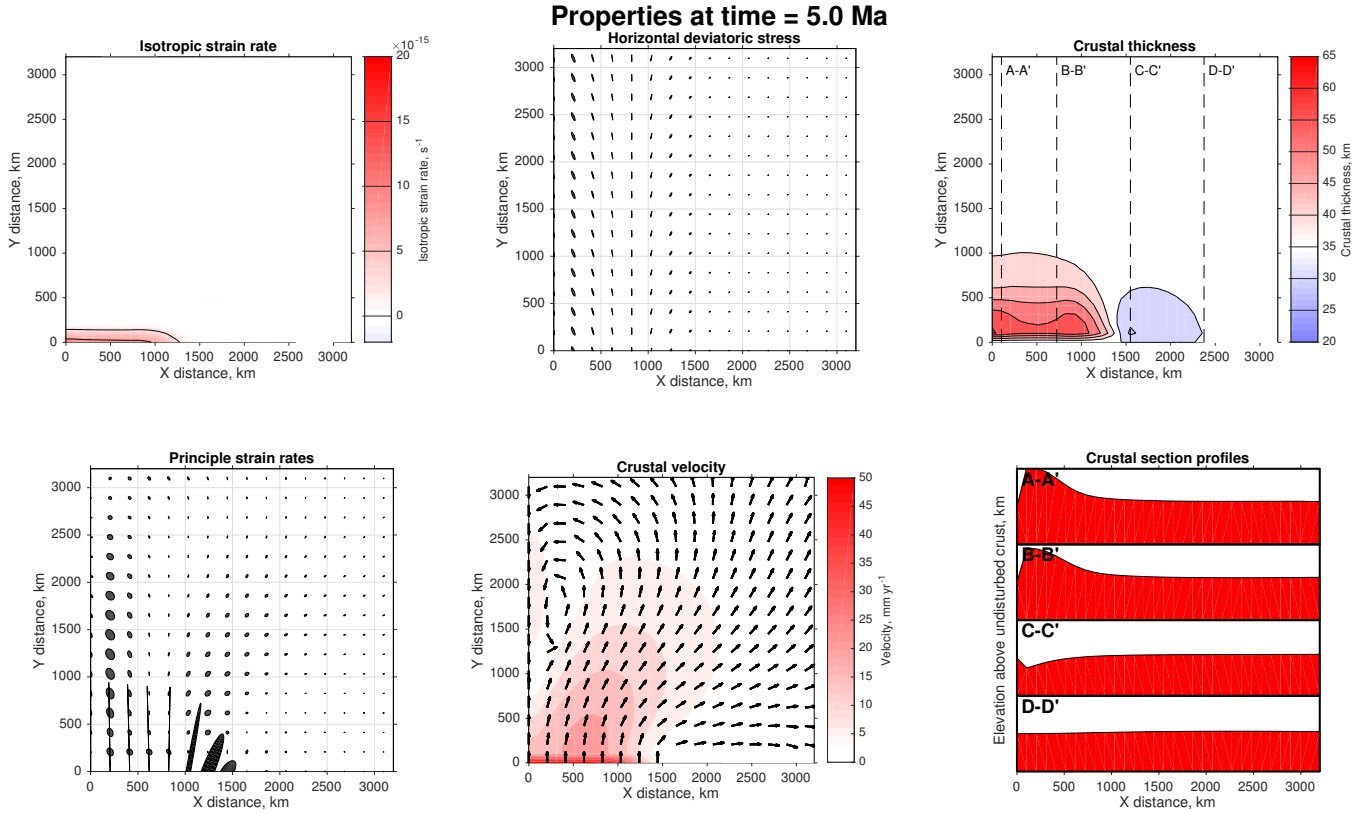

Figure 3: As Figure 2, except performed for 5 Myrs.

High Argand number

High Argand number simulations display a much more dispersive stress and strain field, which is also shown in the wide region of crustal thickening at 5 Myrs (Figure 5). Less crustal thinning is also observed.

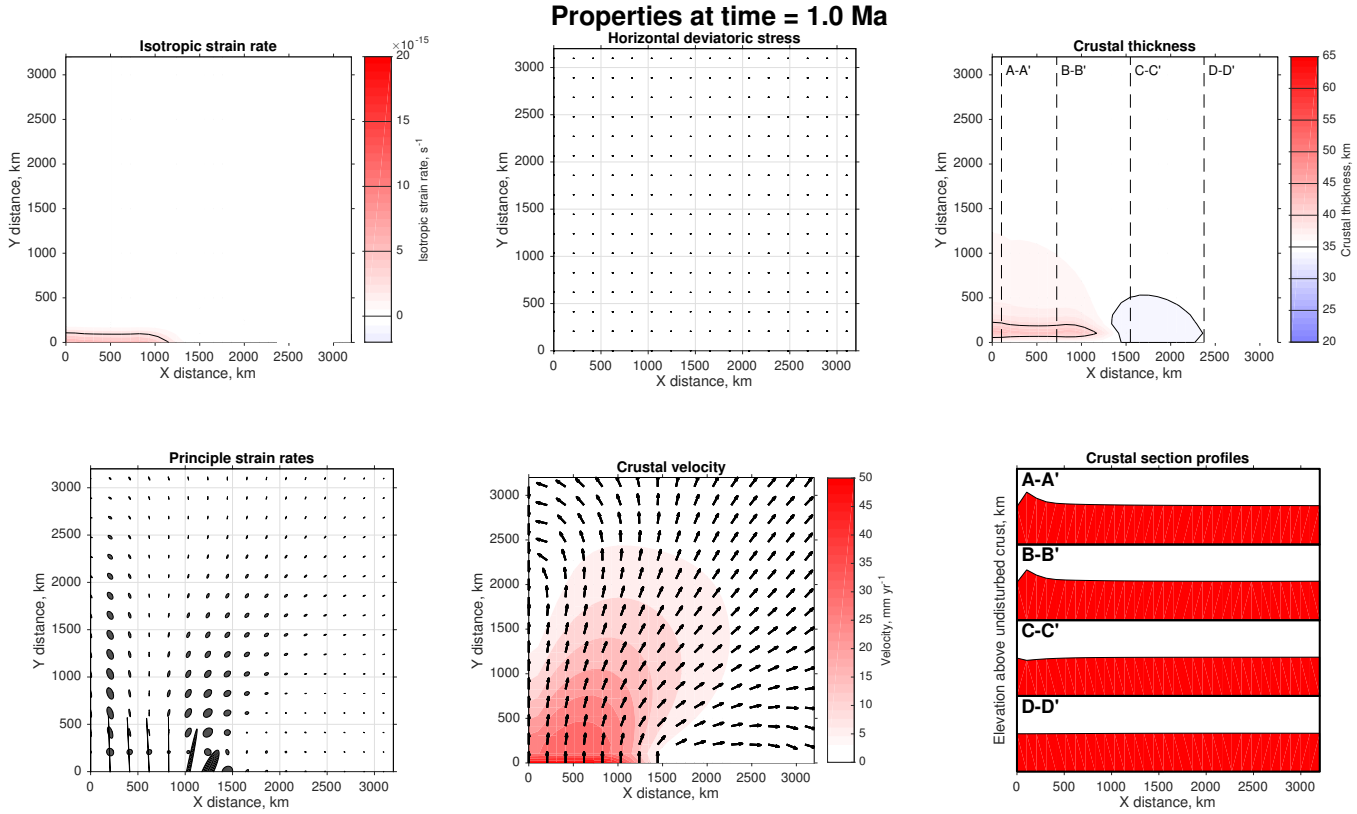

Figure 4: As figure 2, except performed at Ar=10, n=1, for 1 Myrs.

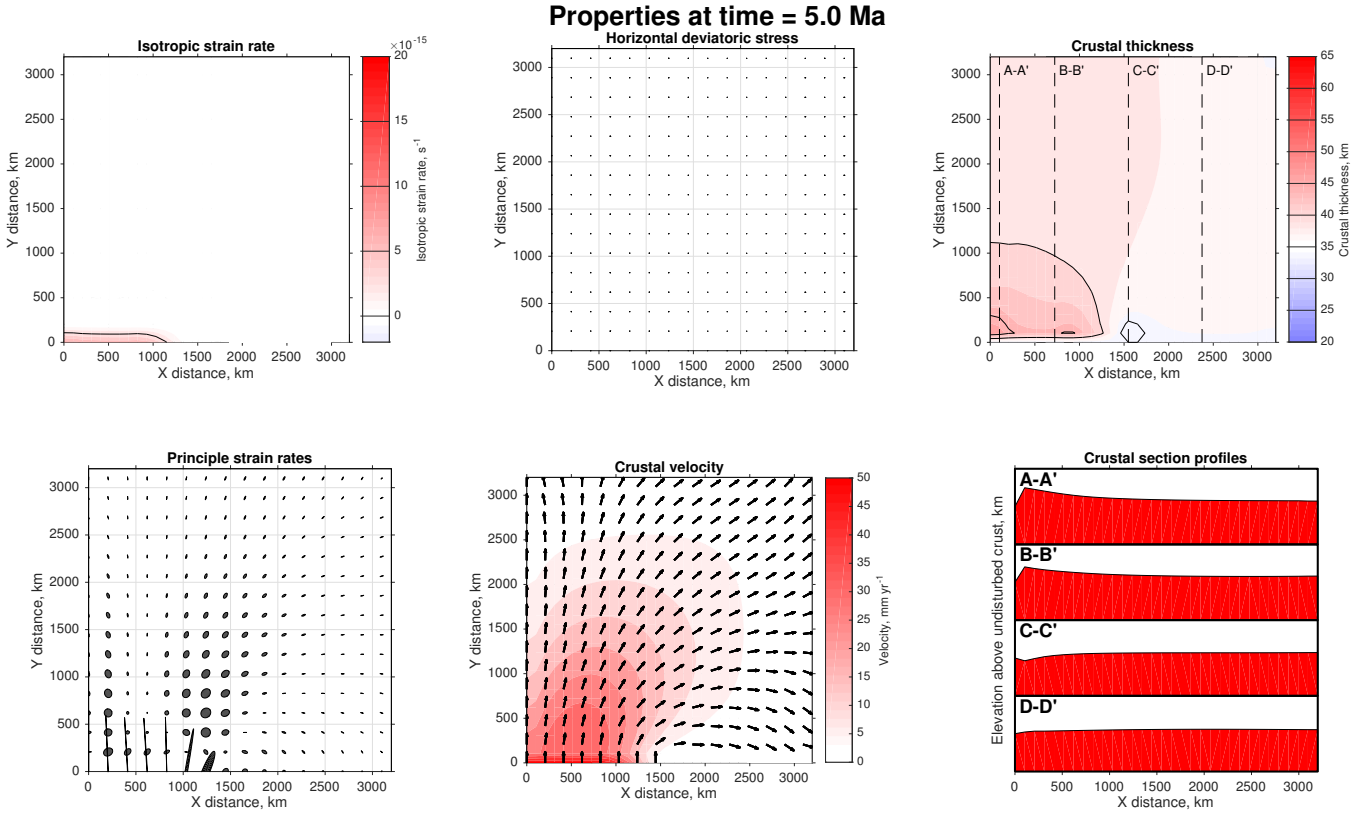

Figure 5: As figure 2, except performed at Ar=10, n=1, for 5 Myrs.

CONCLUSION

This model seems to reproduce the most basic functions of the thin viscous sheet assumption, with low Argand simulations localising deformation and high Ar models dispersing it. It is definitely possible to make estimates about the properties of large scale continental collision regions by comparing models like these to physical and geophysical observations.

Checks should be made with the boundary conditions, as there is a worrying "Southwards" velocity field in parts of Figure 2. Variations in the power law, n, should be investigated in the future.

REFERENCES

[1] Philip England and Dan McKenzie. A thin viscous sheet model for continental deformation. *Geophysical Journal International*, 70(2):295–321, 1982.

[2] Philip England and Dan McKenzie. Correction to: a thin viscous sheet model for continental deformation. *Geophysical Journal International*, 73(2):523–532, 1983.